

# Near Infra-Red Absorption Tomography for Measurement of Chemical Species Distribution

S.J. Carey<sup>1</sup>, H. McCann<sup>1</sup>, D.E. Winterbone<sup>2</sup> and E. Clough<sup>2</sup>

<sup>1</sup>Dept. of Electrical Engineering & Electronics, UMIST, M60 1QD

<sup>2</sup>Dept. of Mechanical Engineering, UMIST, M60 1QD

*HMcC and SJC are members of the Virtual Centre for Industrial Process Tomography*

**Abstract** – *The spatial distribution of chemical species can be a critical determinant of the performance of chemical reactors. One such reactor is the combustion chamber of the Internal Combustion engine. This paper presents a design for the measurement of hydrocarbon concentration distribution within a running engine using Near Infra-Red absorption tomography. The fundamentals of the technique, and design parameters for the equipment are discussed. By utilising micro-optic components, a minimally invasive system is feasible and by utilising advanced laser/photodetector combinations, good temporal performance is anticipated.*

**Keywords:** tomography, combustion, infra-red, spectroscopy

## 1. INTRODUCTION

In many chemical processes of industrial or commercial interest, the relevant reactions take place over extended regions of space with rates that are dependent on factors such as mixture homogeneity or distribution, temperature and pressure. The study of systems containing liquid reactants has shown the benefits of electrical resistance tomography for measurement of species distribution [1].

In cases where there is no contrast due to bulk physical or electrical properties, there are presently very few techniques available to the researcher or process engineer that enable access to the distribution of chemical species.

This paper presents an Infra Red tomography technique that is applicable to the measurement of gaseous hydrocarbon distributions. The measurement of the distribution of gaseous species is of importance for applications such as pollution monitoring and combustion research [2],[3].

The particular application targeted is the measurement of gasoline vapour distribution within the combustion chamber of an internal combustion engine.

### 1.1. Absorption Spectroscopy and Tomography

The transmission of light from a wavelength-swept narrow band source through an unknown chemical species can provide the means for its complete or partial identification, given that the species has a number of identifiable absorption peaks within the wavelength range of the source.

Such absorption peaks often represent functional groups within a molecule [4].

When determining *concentration* of a species known to be present, a wavelength-swept source is generally not required; a single absorbed wavelength can be chosen, with absorption strength relating to concentration. However, other contributions to the received signal (ambient light, contaminant-induced absorption) must be accounted for.

Gaseous species that absorb light in the near infra-red region of the electromagnetic spectrum (1 $\mu$ m to 2.5 $\mu$ m), for example those shown in Table 1, will be amenable to measurement with the techniques and systems developed in this work.

Species	Formula	Absorption $\lambda$ in NIR/nm
nitric oxide	NO	1800
carbon dioxide	CO <sub>2</sub>	1960
methane	CH <sub>4</sub>	1650
water	H <sub>2</sub> O	1390
carbon monoxide	CO	1570
ethyne	C <sub>2</sub> H <sub>2</sub>	1520
long chain HC's – partial saturation	-	1700

Table 1. Species absorbing light in the near infra-red

However, absorption of a single transmitted beam through a gas cloud (Figure 1) only tells us average concentration along a path. If the material is heterogeneous, a large number of different views through the object, followed by tomographic reconstruction, enables the concentration variation within the cloud to be determined. For non-parallel beams with

irregularly placed detectors, algebraic reconstruction techniques (ART) are the most appropriate [5].

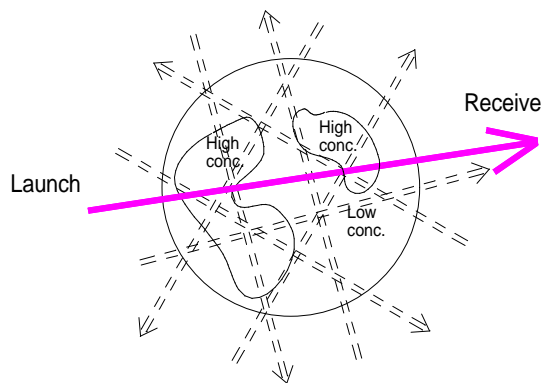


Figure 1. Schematic diagram of transmission paths through a gas cloud of variable concentration, for tomographic reconstruction

## 1.2. Imaging in the Internal Combustion Engine

This paper is concerned with the design of a near infrared tomographic system for the measurement of hydrocarbon concentration distribution within the cylinder of an internal combustion engine. The system will exploit the weak absorption of long chain hydrocarbons at  $1.7\mu\text{m}$  (see Table 1).

The measurement of hydrocarbon concentration within an internal combustion engine provides engine researchers with information on the efficacy of, for example, new combustion chamber designs and fuelling strategies [3], [6]. However, the tools currently available (see section 1.3) require considerable changes to the engine and combustion chamber, suffer from poor temporal performance and are costly. The design proposed here aims to produce an all opto-electronic system that allows flexible and reliable measurements at high image rates.

The target specification of the system is as follows:

- (i) Temporal resolution of 1 frame/ $^{\circ}\text{CA}$  (crank angle) at 2000rpm
- (ii) Spatial resolution of less than  $D/5$ , where  $D$ , the chamber diameter, is approximately 85mm for a typical engine cylinder;
- (iii) Hydrocarbon measurement precision of 5% of stoichiometry at 10 bar.

## 1.3. Existing techniques

Planar Laser-Induced Fluorescence typically exploits detection of fluorescence at  $90^{\circ}$  to the direction of the stimulation beam [3], [7], [8], [9]. Most implementations of this scheme involve the

replacement of part of the cylinder wall with large glass windows through which the stimulant high energy pulsed laser beam is directed in a sheet form. A further window and mirror mounted on an extended piston directs fluorescence from the mixture onto a camera, typically a low-noise CCD array. The implementation of the system is necessarily complex in that the modifications to the engine are very severe. In general, a model single-component fuel is used, usually iso-octane, with fluorescent dopants added, 3-pentanone being most widely used. In addition, data can only be obtained at the repetition rate of the pulsed laser, limited to 100Hz [9], and typically 1Hz.

Previous attempts to monitor gaseous hydrocarbons by absorption [10],[11],[12],[13] have also required large-scale optical access. Flame and soot emission studies [14], [15], [16] generally require the least degree of optical access. The measurements of flame emission clearly do not detect hydrocarbon presence directly; however minimal optical access by inclusion of fibres and micro-optic lenses in the cylinder wall is appealing. The emission study of [16] additionally achieves soot monitoring via monitoring of light at 650nm. However, the lack of simultaneous sampling means that monitoring of hydrocarbon motion within a single cycle is not realised. The repeatability of hydrocarbon combustion from cycle to cycle is of critical importance to engine researchers [17].

## 2. NIR TOMOGRAPHY

In order to achieve good image quality, several competing effects to species-dependent absorption have to be overcome: scattering due to fuel droplets, contamination of optical components and blackbody radiation [12], [13], [16], [18].

### 2.1. Theory

The transmitted light through a distance  $x$ , of a uniformly absorbing material is given by the Beer Lambert Law:

$$(1) \quad I_r(I) = I_o(I)e^{-a(I)cx}$$

where

$I_r(\lambda)$  = received light intensity at  $\lambda$

$I_o(\lambda)$  = launched light intensity at  $\lambda$

$\alpha(\lambda)$  = absorptivity at  $\lambda$

$c$  = molar concentration

In the case considered, where the receiver is operating in an environment of high temperature, blackbody radiation adds to the received signal. In addition, non-resonant absorption must be accounted for by modifying equation (1) as follows:

$$(2) \quad I_r(I) = I_o(I) \cdot e^{-a(I) \cdot L} \cdot F + I_T$$

where  $F$  is the attenuation due to mechanisms which are not specific to the hydrocarbon species of interest, as discussed above.  $I_T$  is the intensity due to thermal background radiation.

When the gas concentration is not uniform, the received light intensity after transmission across a path  $L$  is given by:

$$(3) \quad I_r(I) = I_o(I) \cdot \exp\left(-\int_L a(I)c(x,y)dl\right) \cdot F_L + I_{TL}$$

where  $F_L$  is specific to each particular path (over the time of the measurement) and  $I_{TL}$  is specific to the viewing path of the receiving optics (at the measurement time).

The necessary information for tomographic reconstruction from several path-integrated measurements is contained within the exponent in equation (3). Therefore, the measurement strategy must be designed to determine the above integral.

Using two different wavelengths,  $\lambda_1$  and  $\lambda_2$ , effects common to both wavelengths (i.e.  $F_L$ ) can be removed, leaving a path-concentration integral given by:

$$(4): \quad \int_L c(x,y)dl = \frac{1}{a(I_1) - a(I_2)} \ln\left(\frac{I_r(I_2) - I_{TL} I_o(I_1)}{I_r(I_1) - I_{TL} I_o(I_2)}\right)$$

In general,  $\lambda_1$  and  $\lambda_2$  are chosen such that the chemically specific absorptivity,  $\alpha(\lambda_1)$ , of wavelength  $\lambda_1$  is large due to resonant vibrational/rotational transitions, and the absorption of  $\lambda_2$  is dominated by non-resonant, non-chemically specific attenuation mechanisms i.e.  $\alpha(\lambda_2)$  is small, although  $F_L$  may be significant.  $\lambda_2$  is termed the "reference" wavelength.

Hence, the data we require from each beam track are the launch powers at each wavelength (which should be constant over a long period), updated values of received power at each wavelength and a value for blackbody radiation. The received light values at each wavelength should be collected simultaneously for all beam tracks.

## 2.2. System considerations and technologies

Within the near infra-red wavelength region, there are a number of available technologies:

**Fibres:** Silica fibre is useably transmissive for fibre optic sensors between 300nm and 2100nm (attenuation staying below 0.1dBm<sup>-1</sup>). Hence this is the fibre of choice.

**Detectors:** Available detectors in the near infrared are shown in Table 2. Detectivity is given at 1.7µm for relevance to this work.

Detector technology	D* at 1.7µm at 20°C [cmW <sup>-1</sup> Hz <sup>1/2</sup> ]	Operating λ/nm
Ge	3.0·10 <sup>10</sup>	700-1800
InGaAs (IGA)	<sup>(1)</sup> 8.0·10 <sup>11</sup>	800-1700
Extended IGA InGaAsSb/InAsSbP	2.0·10 <sup>11</sup>	1000-2100 or 2500
InAs	5·10 <sup>8</sup>	1000-3800
PbS	4·10 <sup>10</sup>	1000-3300
PbSe	5·10 <sup>9</sup>	1000-4500
InSb	2·10 <sup>10</sup> (77K)	1000-5500

(1) assumes 0.15A/W responsivity

**Table 2. Detector options for near infra-red**

For the purposes of this work, IGA and extended IGA devices appear to offer the best performance prospects.

**Multiplexing/De-multiplexing:** the transmission at each of the two wavelengths for each beam track must be determined at the receivers. This can be made possible by optical wavelength de-multiplexing onto separate photodiodes, or, by wavelength encoding by means of time division or frequency multiplexing. Techniques for the former (optical de-multiplexing), and attributes, are as follows:

1. Multi-layer filters - expensive since lens/filter assemblies are also required;
2. Fibre-optic fused biconical taper couplers – expensive; poor isolation if wavelengths close; lossy since single mode fibre must be used;
3. Multi-mode fibre WDM – lossy;
4. Integrated optic fibre components – expensive;
5. Spatial filtering - requires two launch systems; expensive; potential deleterious effects on reconstructed image.

Of these techniques, a bespoke multi-mode WDM may be the most cost-effective solution. However, all solutions would require a second array of detectors and would result in a lack of flexibility and upgradeability in laser wavelength. Hence electronic multiplexing in frequency or time domains is favoured.

**Lasers/LEDs:** Since we have a requirement to modulate the sources, there are a number of options:

1. Diode lasers – using amplitude modulation via the drive current;
2. OPO lasers – choosing an appropriate pulse repetition frequency;
3. Gas lasers - with an external amplitude modulator.

At present, the spectral shapes of LED sources are too broad for this application, although work underway with resonant cavity-enhanced LEDs is promising [19]. Ideally, the spectral characteristics of IR sources should be selected with respect to linewidth as well as central wavelength; too narrow a linewidth can lead to system instabilities related to etalon/speckle effects [11] and to species temperature/pressure change through spectral broadening.

Ease of use, cost, power output and linewidth require use of a diode laser. Such devices are generally available from 630nm to 2000nm. However, there are notable gaps in the range: 1100-1250nm, 1350-1440nm and 1670-1750nm. These gaps are gradually being filled as semiconductor technology develops. A customised 1700nm laser is being manufactured for this project.

### 3. INFRA-RED ABSORPTION IN A COMBUSTION ENVIRONMENT

The primary fuel considered in this study is iso-octane (2,2,4 tri-methylpentane). The absorption lines utilised in previous studies were 3.4 $\mu\text{m}$  [10],[12] and 2.3 $\mu\text{m}$  [13]. This study proposes the use of the second harmonic of the C-H stretch mode at 1.7 $\mu\text{m}$ . Spectra are generally available for liquid phase species [20],[21]; less so for the gaseous phase. Using a single channel sample cell built at UMIST (Figure 6), the spectral absorbance of gaseous iso-octane in the wavelength region of interest was determined (however, independent calibration of vapour concentration has not been completed at the time of writing). This yields the absorption spectrum for a typical path in an internal combustion engine as shown in Figure 2. The peak absorption wavelength occurs at 1700nm. Whilst the linewidth of this peak is dominated by absorption effects, the linewidth of the source prevented determination of any potential fine structure in the spectroscopy of the gas. This remains a matter for further study.

Studies of the variation of iso-octane absorption with temperature and pressure are underway. Some preliminary sample data are shown in Figure 3.

The requirement for the reference wavelength is that it should be largely unabsorbed by both the measured species and other species that may be present in the combustion chamber i.e. primarily water and carbon dioxide. Utilising the USAF's Modtran 3.7 software and database allows an insight into the likely absorption resulting from these species as shown in Figure 4 and Figure 5. From this data it appears that a

wavelength between 1500nm and 1670nm would be suitable as a reference.

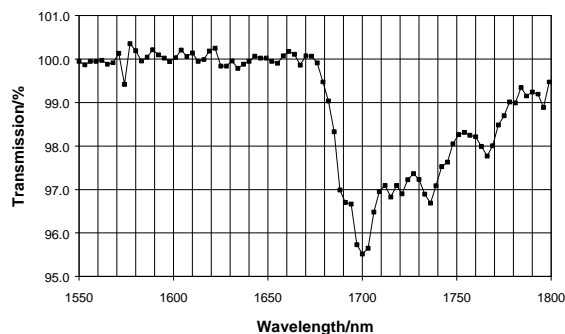


Figure 2. Transmission of gaseous iso-Octane. 10 bar, 80°C, stoichiometric mixture with air. 85mm path length. 5nm source bandwidth. Normalised to 100% transmission at 1650nm.

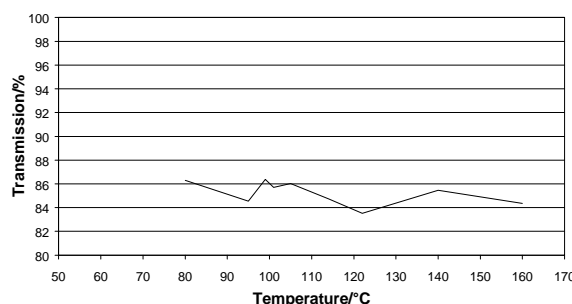


Figure 3. Peak absorption of gaseous iso-octane at 1700nm with changing temperature (at pressure of 1bar). 5nm source bandwidth. 164mm path length. 0.0073moles.l<sup>-1</sup> concentration.

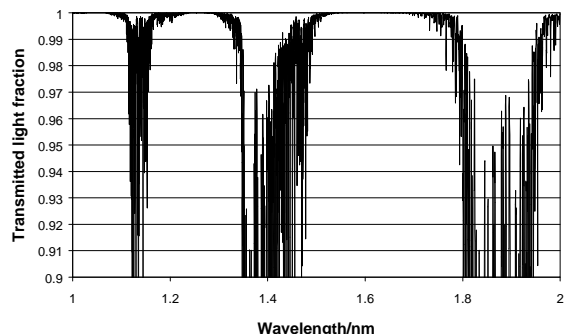


Figure 4. Light transmission for water. Concentration 134000ppm, 85mm path length, 1cm<sup>-1</sup> source resolution, 10 bar, 500°C.

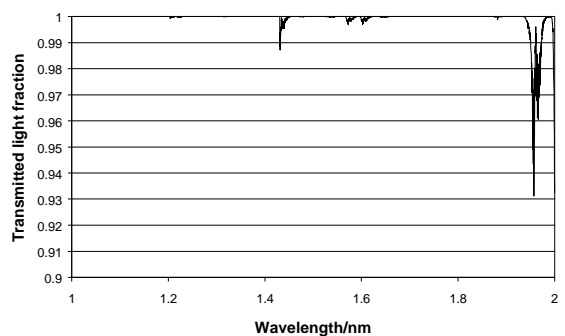


Figure 5. Light transmission for carbon dioxide. Concentration 119000ppm, 85mm path length, 1cm<sup>-1</sup> source resolution, 10 bar, 500°C.

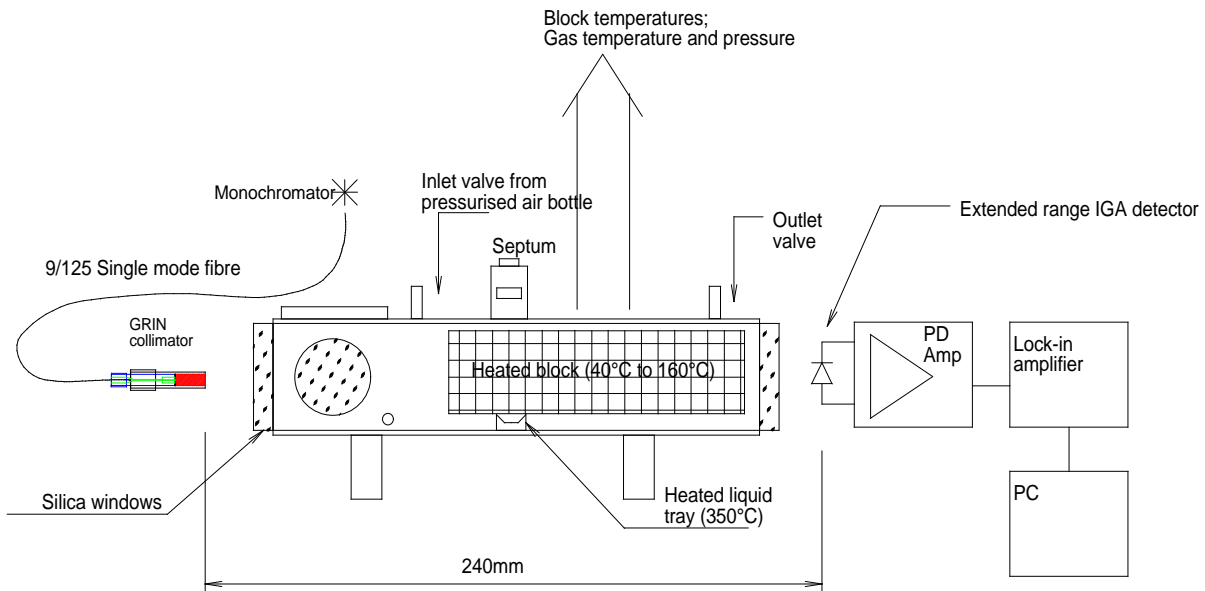


Figure 6. Pressurised chamber for gaseous spectral absorption analysis

## 4. INSTRUMENT ARCHITECTURE

### 4.1. Optical system design

The proposed system architecture is shown in Figure 7. The system design (to the point of light reception) attempts to utilise many components primarily designed for telecommunications (couplers, fibres, photodiodes). The aim of the opto-electronic design is to achieve adequate signal to noise in terms of the integrated concentration along a path. For use in ART image reconstruction, the signals must in turn meet the noise requirement for the reconstructed image (see required specification).

For the purposes of illustration, we assume here that the thermal background is negligible, and errors in determining the path integral are dominated by the noise in the received photocurrent. In addition, we assume that both wavelengths are launched into the gaseous subject by each fibre; they are coded and demultiplexed in the frequency domain (FDM).

Since the absorption is low, the prime noise component (given effective receiver design) should be related to the shot noise arising from the received light (given equal photocurrent contributions from each source):

$$(5) \quad i_n = \sqrt{2eLi_s B}$$

where,

$i_s$  = photocurrent due to each laser

$B$  = bandwidth

$e$  = electron charge

$i_n$  = noise current

$L$  = number of lasers

The signal to noise ratio in the calculated path-concentration integral,  $N_{PCI}$ , is approximately half that of the individual signal to noise ratios of the two signals:

$$(6) \quad N_{PCI} = \frac{i_s A_\lambda}{i_n 2}$$

where

$A_\lambda$  = absorption at  $\lambda$  ( $i_s A_\lambda$  represents the useful signal within a single measurement)

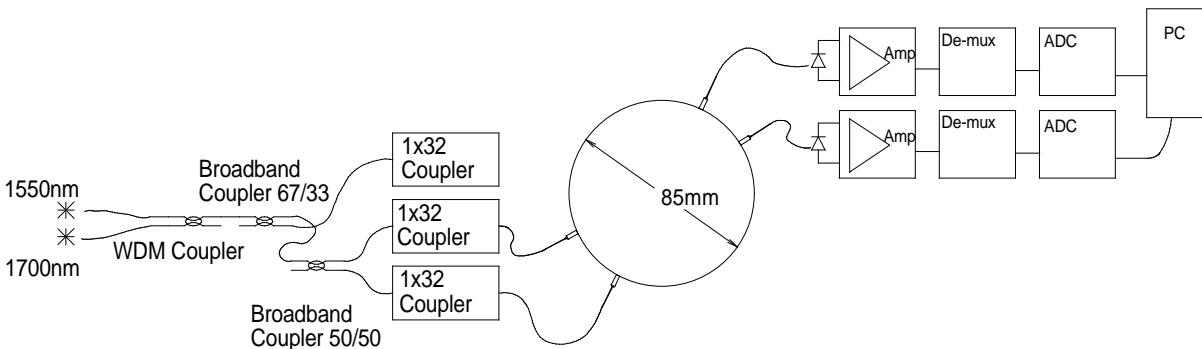


Figure 7. Optical tomography system design

Given that we know the required signal to noise ratio of the reconstructed image,  $N_{RI}$ , from the specification, we can estimate  $N_{RI}$  in terms of the signal to noise of the path-concentration integral, assuming some degradation due to demultiplexing and reconstruction:

$$(7) \quad N_{RI} = N_{PCI} \frac{1}{RD}$$

where,

$R$  = reconstructed pixel noise as function of electronic noise, estimated to be 2;  
 $D$  = factor increase in noise due to demultiplexing, estimated to be 2.

Hence a value for the received photocurrent required is approximated to:

$$(8) \quad i_s = 4.e.B \left( \frac{L.N_{RI}.R.D}{A_I} \right)^2$$

Given  $B=10\text{kHz}$ ,  $L=2$ ,  $A_i=0.045$ ,  $N_{RI}=20$ ,  $R=2$  and  $D=2$ , the required photocurrent is 81nA.

This is clearly an approximation - in particular the factor increase in noise due to reconstruction can only be determined to any accuracy given detailed knowledge of the system to be measured. The demands on the front-end electronics are significant since at these signal levels, the amplifier voltage noise of the photodiode amplifier can dominate. However, significant out of band noise originating from voltage noise can be removed by use of a lock-in amplifier (LIA) which acts as a very high quality bandpass filter. Noise modelling of the photodiode amplifier has demonstrated the requirement for lock-in detection for removal of noise. The performance of a typical design for a photodiode amplifier is shown in Figure 8. The cause of the rapid increase in noise after the cut-off is due to gain peaking of the amplifier voltage noise component. This has a different bandwidth to that of the signal but is not coupled beyond the LIA stage.

Given the signal requirement, the power budget in Table 3 is determined:

<b>Rx power given <math>\eta = 0.15\text{A/W}</math></b>	<b>-32.7 dBm</b>
Coupling to detector	-1.5 dB
Link loss (via cylinder)	-3.5 dB
1x32 coupler	-19 dB
Broadband couplers	-6 dB
WDM loss	-1 dB
<b>Laser power required (in fibre)</b>	<b>-1.7 dBm</b>

Table 3 Power budget for 95 channel system given 81nA signal power required.

This shows that with a fibre-coupled power of 680µW, the system requirements are achievable.

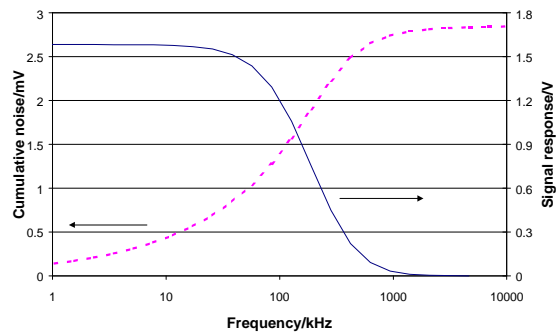


Figure 8. Frequency and cumulative noise response of a photodiode amplifier of bandwidth 100kHz

#### 4.2. Photodetectors

Requirements of the photodetector for this application are to:

1. Show good responsivity at 1700nm
2. Couple with high efficiency from large core receiving fibres.
3. Have low capacitance (and hence low noise and high bandwidth)
4. Have low cost (due to their significant number)

The responsivity issue is of particular concern since IGA photodiodes (designed for telecommunication applications) cease to be responsive around 1700nm. A number of devices were characterised as shown in Figure 9.

Suitable photodiodes are extended IGA devices or, at the margin, selected standard IGA devices. The latter have the advantages of:

- lower capacitance (and hence higher bandwidth);
  - higher shunt resistance;
  - low cost;
- and the following disadvantages:
- high temperature sensitivity at 1700nm;
  - lack of response above 1700nm to allow for system upgrades and changes.

Hence the final choice of photodiode is finely balanced; to allow for prototype development, extended IGA diodes are preferred.

#### 4.3. Multiplexing System

There are a number of options for signal coding including frequency division multiplexing (FDM), time division multiplexing (TDM) and optical filtering of signals (see section 2.2). Of these, the most appealing is FDM (Figure 10), since it enables lock-in detection to be utilised at the receiver as discussed above. This in turn enables the lowest noise coupling and incorporation of anti-aliasing filters (which would be more difficult to incorporate in a TDM system). A system design for TDM also requires the incorporation of a method of measuring

thermal background radiation. For FDM, thermal background is automatically removed if modulation frequencies are chosen carefully;

however thermal emission is a useful measurand in itself if flame emission is to be measured.

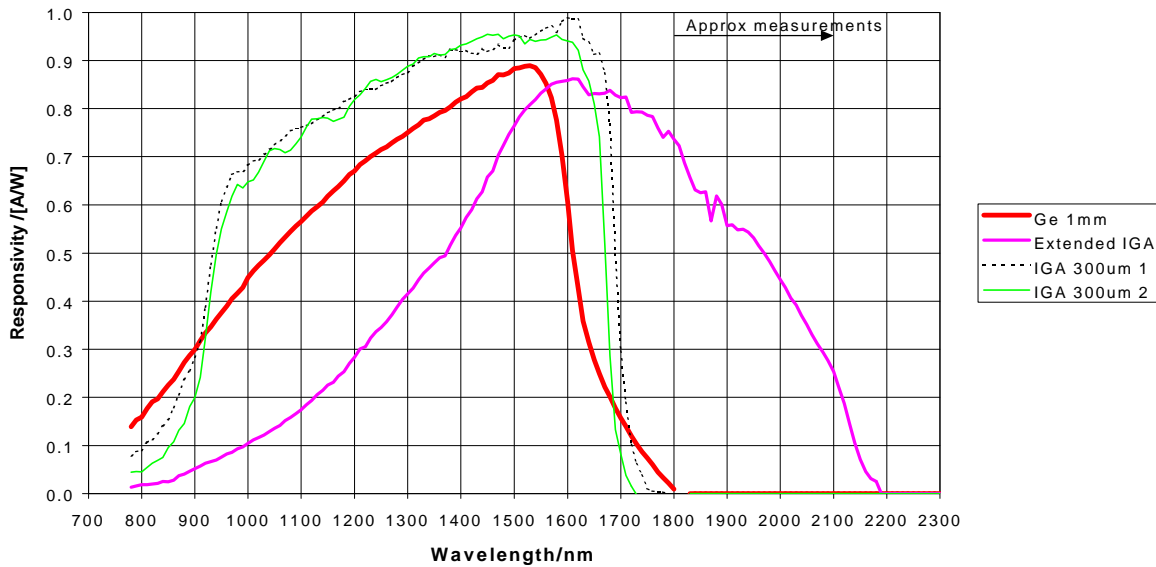


Figure 9 Responsivity of Photodiodes

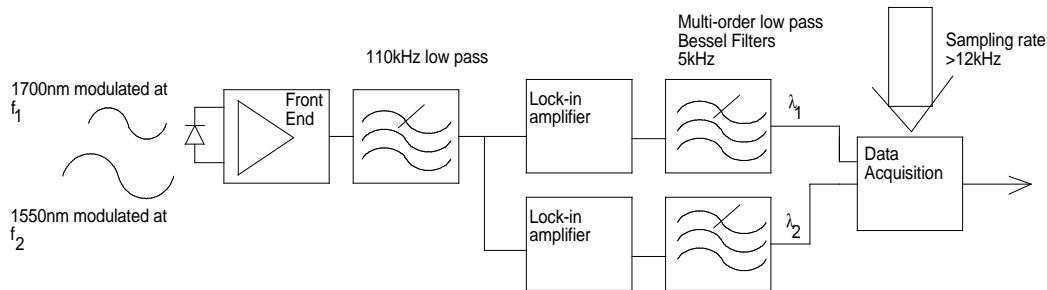


Figure 10. Demultiplexing scheme

#### 4.4. Opto-mechanics

The manner in which the optical components can be assembled to allow access to a combustion chamber is critical to the system's success. Figure 11 shows a system incorporating 28 channels. Work is underway to increase this number. A particular challenge in this regard is the physical space available for the total of 190 launch and receive fibres which appear to be feasible from power budget calculations. Use of fan beam optics [11] will reduce this number but at the expense of higher insertion loss.

#### 5. CONCLUSIONS

A near infra-red tomography system has been designed for the sensing of hydrocarbons in a combustion environment. It is believed that an effective system can be built in spite of weak absorption at the selected wavelength of 1.7µm. Using components designed for the telecommunications industry will enable a cost-

effective all opto-electronic solution to be implemented. Problems still exist due to space constraints around an 85mm diameter cylinder.

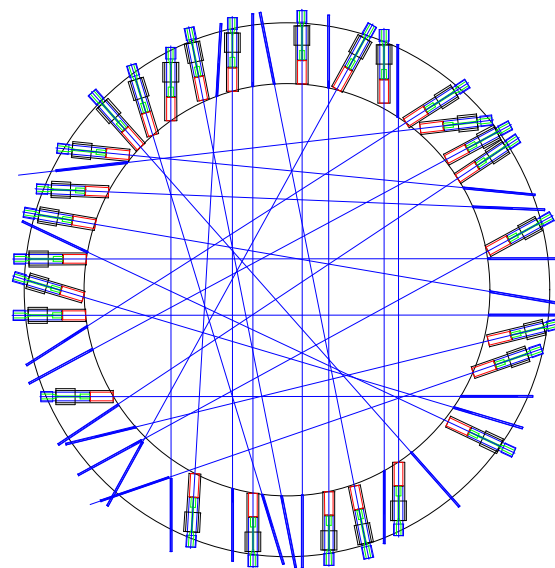


Figure 11. 28 channel system

## ACKNOWLEDGEMENTS

The support of EPSRC is acknowledged via GR/L67592. The authors are grateful for helpful discussions with Stan Wallace (Rover Group), Steve Nattrass (Shell Research) and Frank Hindle (UMIST).

## REFERENCES

- [1] P.J. Holden, M. Wang, R. Mann, F.J. Dickin, R.B. Edwards, "Imaging stirred-vessel macromixing using electrical resistance tomography", *AIChE Journal*, April 1998, Vol.44, No.4, pp.780-790
- [2] R. Grisar et al (Eds) "Monitoring of Gaseous Pollutants by Tunable Diode Lasers", 3<sup>rd</sup> International Symposium Oct. 1991. Kluwer, Dordrecht (1992)
- [3] M Berckmuller, N.P. Tait, D.A. Greenhalgh, "The Time History of the Mixture Formation Process in a Lean Burn Stratified-Charge Engine", SAE 961929.
- [4] H.A. Szymanski, "Interpreted Infrared Spectra", Plenum, New York (1964)
- [5] R.G. Jackson, "The Development of optical systems for process imaging" in "Process Tomography – Principles, Techniques and Applications" (Eds. R.A. Williams, M.S. Beck), 1995, Butterworth-Heinemann
- [6] "Direct Injection SI Engine Technology", SAE SP-1314, Warrendale USA, 1998.
- [7] D.A. Greenhalgh, "Optical Diagnostics for flow processes", Eds L. Lading, S. Wigley and P. Buchhave, Plenum Pub. Corp., NY, 1994 and references therein.
- [8] F. Hildenbrand, C. Schultz, V. Sick, G. Josefsson, I. Magnusson, O. Andersson, M. Alden, "Laser spectroscopic investigation of flow fields and NO<sub>x</sub> formation in a realistic SI engine" SAE Special Publications, Feb 1998, Vol.1348, pp.107-116 ("Analysis of Combustion and Flow Diagnostics")
- [9] E. Winklhofer, H. Fuchs, "Laser induced fluorescence and flame photography - tools in gasoline engine combustion analysis", *Optics and Lasers in Engineering*, Dec 1996, Vol.25, No.6, pp.379-400
- [10] H. Kawazoe, K. Inagagi, Y. Emi, F. Yoshino (1997) "Computer Tomography Measurement of Gaseous Fuel Concentration by Infrared Laser Light Absorption", SPIE Vol. 3172, pp576-584
- [11] E.J. Beiting, (1992), "Fibre-optic fan-beam absorption tomography", *Applied Optics*, Vol. 31, p. 1328
- [12] E. Winklhofer, G.K. Fraidl, A. Plimon (1992), "Monitoring of gasoline fuel distribution in a research engine", *Proc. I.Mech.E.* Vol 206, p.107.
- [13] S.M. Skippon, S.R. Nattrass, J.S. Kitching, L. Hardiman, H. Millar, "Effects of fuel composition on in-cylinder air/fuel ratio during fuelling transients in an SI engine, Measured using differential infrared absorption", SAE 961204
- [14] U. Spicher et al, "Application of a new optical fibre technique for flame propagation diagnostics in IC engines", SAE 881637
- [15] H. Philipp, A. Plimon, G. Fernitz, A. Hirsch, G. Fraidl, E. Winklhofer, "A Tomographic Camera System for Combustion Diagnostics in SI Engines", SAE 950681
- [16] A.E.M. Barrag, B. Lawton, "Computer optical tomography in the study of internal combustion engine soot concentration", 26<sup>th</sup> international symposium, Automotive technology and automation, Vol.: "The motor vehicle and the environment – demands of the nineties and beyond", Sept. 1993, Aachen.
- [17] J.B. Heywood, "Internal Combustion Engine Fundamentals", (McGraw-Hill, 1988)
- [18] S.R. Nattrass, D.M. Thompson, H. McCann, "First In-Situ measurement of lubrication degradation in the ring pack of a running engine", SAE 942026.
- [19] B.M. Poole, K.E. Singer, M. Missous, "Wafer Bonded Resonant-Cavity Light-Emitting Diodes for 1.7 $\mu$ m emission", submitted to Conference of Postgraduate Research in Electronics, Photonics and related fields 1999, Manchester.
- [20] M. Buback, H.P. Vogele, "FT-NIR Atlas", (VCH, Germany)
- [21] "The Atlas of Near Infrared Spectra" (Sadler/Heyden, Philadelphia/London, 1981)